

PAPER • OPEN ACCESS

Analysis of microwave-readable RFTES bolometer

To cite this article: A V Merenkov *et al* 2019 *J. Phys.: Conf. Ser.* **1182** 012009

View the [article online](#) for updates and enhancements.



IOP | ebooks™

Bringing you innovative digital publishing with leading voices to create your essential collection of books in STEM research.

Start exploring the collection - download the first chapter of every title for free.

Analysis of microwave-readable RFTES bolometer

A V Merenkov¹, V I Chichkov¹, A V Ustinov^{1,3} and S V Shitov^{1,2}

¹ National University of Science and Technology MISiS, 119049, Moscow, Russia

² Kotel'nikov Institute of Radio Engineering and Electronics, 125009, Moscow, Russia

³ Physical Institute, Karlsruhe Institute of Technology KIT, 76131 Karlsruhe, Germany

sergey3e@gmail.com

Abstract. We demonstrated and analyzed the smooth microwave-driven transition of a superconducting bridge made from Hf into its normal state at bath temperatures below the critical temperature of Hf ($T_c \approx 380$ mK). The bridge is integrated on a silicon chip with both the 600-700 GHz double-slot antenna and the 1.5-GHz CPW quarter-wave resonator (Q-factor $\sim 10^4$) made from 100-nm Nb film. The experimental bridge was sized 2.5 μm by 2.5 μm by 50 nm and tested at temperatures down to 50 mK. Similar to the technique of MKID, we measured the dependence of transmission S_{21} on microwave power at the bottom of the resonance curve. It was found that the microwave power absorbed in the bridge fits to the model of hot electron gas, $P \sim T_e^6 - T_{\text{ph}}^6$. The internal NEP down to $\approx 10^{-18}$ W/ $\sqrt{\text{Hz}}$ is estimated due to thermal noise at the optimum electron gas temperature, $T_e \approx 320$ mK. The NEP can be scaled down below $\approx 10^{-19}$ W/ $\sqrt{\text{Hz}}$ via reasonable reduction of the bridge volume. The new detector circuit is suitable for integration within a large imaging array exploiting the FDM-readout.

1. Introduction

The monolithic bolometers are of great interest due to their mechanical and electrical stability. A solution, which is an alternative to the membrane-supported absorber, can be found with the idea of the electron gas absorber [1-2]. Due to slow electron-phonon interaction, the electron subsystem can absorb a terahertz photon and reach its internal thermal equilibrium prior to transfer of the energy to the lattice and down to substrate as it were a mechanically suspended system. In the case of hafnium film, it is possible to achieve such regime within a nano-volume absorber, which is sputtered directly to a dielectric substrate [3]. It was demonstrated that the growing electron temperature can lead to the growing *DC* resistance, if temperature of a superconducting film is set at the transition edge at about T_c , promising *NEP* down to $\approx 10^{-20}$ W/ $\sqrt{\text{Hz}}$ [4-5]. However, a low-noise measurement of the *DC* (low-frequency) impedance is rather difficult, not to mention need in costly SQUID-amplifiers. This is why the readout of such electron gas impedance at a microwave frequency can be beneficial, especially for the implementation of *array* detectors using the method of wide-band frequency division multiplexing (FDM) [6-7].

The FDM circuitry is based on high-Q resonant filters, which provide individual frequency slot for each pixel. This allows for using fewer interface wires that is beneficial for saving cryogenic cooling power. At microwave range, an FDM system has to be designed using one of the existing RF standards (for example, 50- Ω) and can use off-shelf GHz-range microwave amplifiers. Another benefit of an RF standard is the ultimate accuracy of design in respect to the circuit stability. In this case, the



FDM circuit can be a part of the monolithic detector array. This convenience is demonstrated with the rapidly developing microwave kinetic inductance detectors (MKID) [7-9]. Their readout principle is based on probing the reactive part of photon-excited response of a high-Q micro-resonator, which is optimized for ultra-low loss impedance $\sim 10^{-3} \Omega$. Since the recombination time of quasiparticles at millikelvin temperatures is long enough, there is no need for a thermal suspension. This is somewhat similar to the electron gas regime. However, the phase readout of MKID is jitter-sensitive, while the probing power must be non-invasive due to unwanted dark excitations and the existing sensitivity limit for low-energy photons.

Recently, we have designed and tested a new superconducting integrated circuit exploiting the high-Q microwave resonator, which can adopt a much higher impedance, $\sim 1 \Omega$, as shown in Figure 1 and Figure 2. The resonator is loaded with a bridge made from a lower T_c superconductor, which is assumed to exhibit the transition from superconducting to resistive state similar to TES [10-12]. However, one has to expect an essential difference. It is known that near T_c the gap energy $\Delta \rightarrow 0$, so GHz-range photons are breaking Cooper pairs, and the bridge must demonstrate its normal state resistance, which is insensitive to either microwave current or temperature. For this reason, our microwave circuit can neither operate nor respond as HEDD [4-5]. If the operation (bath) temperature is set below T_c , the gap energy, $\Delta \neq 0$, and one may expect the gradual thermal activation of quasiparticles due to growing microwave power. Such regime of microwave probing is invasive at the same time. The electron gas behaves like a non-equilibrium thermometer. The probing current is rising temperature of the electron gas in the bridge above that of the heat sink to reach the optimum impedance, and the incident signal provides an incremental current that results in further rise of the loss in the bridge. To emphasize the microwave nature of the approach, we call it RFTES detector [13-17].

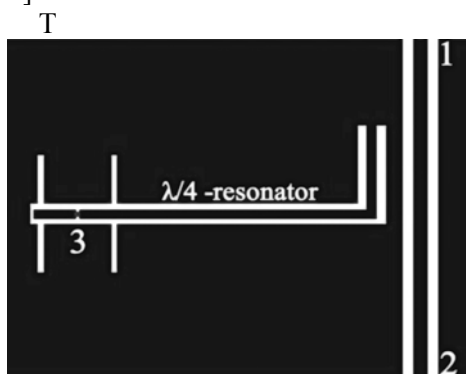


Figure 1. Simplified layout of RFTES chip with double-slot THz antenna integrated with the resonator; ports 1, 2 and 3 explained in Figure 2.

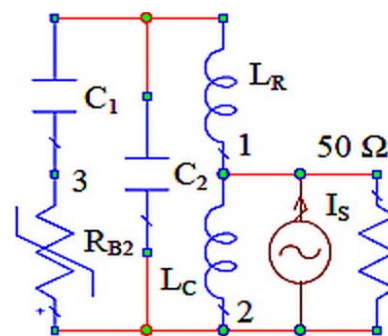


Figure 2. Equivalent scheme of RFTES detector probed with a 50- Ω source at ports 1 and measured at port 2 of a throughput line; the resonator is loaded with absorber R_{B2} at port 3.

To verify approaches to EM-design of RFTES, we have designed and tested a prototype structure at 1.5-5 K. The prototype bridge was made from a very thin film of Nb. It was found that both the resonance frequency and coupling efficiency are fitting the design, and such detector can operate at the optical $NEP \sim 10^{-14} \text{ W}/\sqrt{\text{Hz}}$ [13]. Later the scalable regime of pulsed noise was found [14]. The FDM capability was also tested successfully using the 4-K seven-pixel prototype at 5-8 GHz [16]. In all above cases the invasive measurement was used, so the term “bias power” instead of “probing signal” is more suitable for our experiments. Prior to the ultra-low temperature experiments described below, we have analyzed the possible microwave impedance of hafnium films using the Mattis-Bardeen theory and estimated the range of acceptable probing frequencies [17]. In present report we analyzed the response of the Hf bridge to the bias power at 1.5 GHz, predicting the detector gain and arguing on its NEP potential among the best of its kind.

2. Experimental details and discussion

The experimental samples are tested in the dilution cryostat [18] at temperatures 50-330 mK in the microwave power range $P_{bias} = -105 \dots -75$ dBm (referenced to the chip). Figure 3 illustrates the set of initial experimental data and definition of the value "min. S_{21} " of the resonant curve that is the normalized dip in microwave power measured in arbitrary units (near the center of circled dip in the inset). Since this point is of special interest, in the text below, for simplicity, we use " S_{21} " instead of "min. S_{21} ". It is found smooth, stable and hysteric-free variation of S_{21} vs. applied bias power. Let us state here our basic concept that the loss in the bridge depends on electron gas temperature, T_e , only, meaning that $Q = Q(T_e)$ and $S_{21} = S_{21}(T_e)$. The dependence of the active part of the bridge impedance on the electron temperature, $R_B = Re(Z(T_e))$, was derived from variations of the measured Q -factor.

To extract the data of the non-linear impedance, the exact layout of the chip as in Figure 1 and its equivalent scheme as in Figure 2 have been evaluated using commercial AWR software [19]. The successful fitting of the numerical models to both the experimental layout and $S_{21}(f)$ is a complex procedure deserves to be published in most details elsewhere. The readout circuit of a RFTES, similarly to MKID, is a power-to-power converter: the photon energy is collected at the absorber and delivered at the output of the chip as the increment of the microwave bias power. Since a buffering LNA always adds some noise, the detector with gain is desired. To calculate the conversion efficiency from our variable-bias experiment presented in Figure 3, we have extracted incremental powers, which can be treated as input and output signals under the condition $P_{bias} = const.$

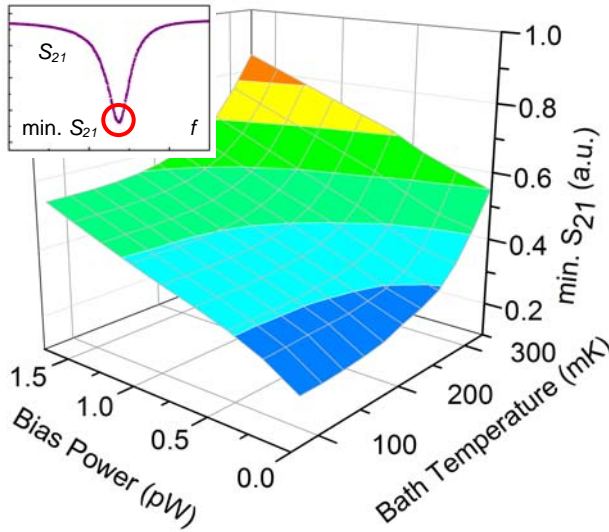


Figure 3. The three-dimensional presentation of experimental data. The surface is a collection of the lowest points of the resonance curve S_{21} at frequency 1.5 GHz, which is shown in the inset. The resonance curve is transformed due to both the microwave bias power, P_{bias} , applied to the chip and the bath temperature, T_{bath} . For reasonably small signals, the curve changes in its amplitude and width (the Q -factor of the loaded resonator), but not in the frequency position. The inset illustrates definition of the lowest point of the resonance curve denoted as "min. S_{21} (a.u.)".

In our experiments, the circuit responds to the growing bias power with growing transmittance, $S_{21}(Z_B)$, that is the result of growing absorption in the bridge, $S_{31}(Z_B)$. The equivalents of input signal power, P_{in} , and the output power, P_{out} , can be found via balance of the total power at the bridge, P_B , and the total power at input of the low-noise amplifier, P_{LNA} :

$$dP_B = P_{in} + P_{bias} dS_{31} = d(P_{bias} S_{31}) \quad (1),$$

$$dP_{LNA} = P_{out} + S_{21} dP_{bias} = d(P_{bias} S_{21}) \quad (2).$$

Here right parts of both equation (1) and equation (2) are extractable experimental data. Defining the power-to-power conversion as

$$Gain = \frac{P_{out}}{P_{in}} \quad (3).$$

and noting that the electro-thermal feedback dS_{31} cannot be a part of signal power, i. e. $dS_{31} = 0$ in equation (1), and, similarly, the bias variation cannot be a part of output signal, i. e. $dP_{bias} = 0$ in equation (2):

$$Gain = \frac{P_{bias} dS_{21}}{S_{31} dP_{bias}} \quad (4).$$

It is worth to note here that the gain reaches its maximum for relatively low R_B with peak right below the embedding impedance of the bridge, $R_s \approx 2.7 \Omega$. This was qualitatively predicted in previous paper [15]. For $R_B > R_s$ the gain is relaxing to about unity as it should be for a normal TES in presence of electro-thermal feedback (ETF) [10]. At this point we have to explain why the gain (3) calculated from equation (4) is dependent on bath temperature.

Referring to the hot electron gas model of Hf described in paper [3], we have fitted the bias power absorbed by the bridge in our experiment, P_B , to the electron temperature, T_e , using the following formula

$$P_B = \Sigma \cdot V \cdot (T_e^6 - T_{ph}^6) \quad (5)$$

as presented in Figure 4. Here $V = 0.75 \cdot 10^{-18} \text{ m}^3$ is the total volume of the experimental Hf film including both the bridge and its overlap with Nb electrodes that gives extra factor $\times 2.4$. The best fit material parameter $\Sigma = 17.5 \cdot 10^8 \text{ W}/(\text{m}^3 \cdot \text{K}^6)$ is of the same order as used in the paper [17]. We neglect here the effect of Kapitza thermal resistance and set $T_{ph} = T_{bath}$. To define $T_e = const$, we used the novel method of steady Q -factor ($Q = const$, $S_{21} = const$) at different T_{bath} . These data were initially measured adjusting P_B for $Q = const$ as described in [17], but later it have been interpolated from general data as $S_{21} = const$ using Figure 3. According to previous equation (4), the gain must grow with growing P_{bias} [15], but this rise is limited, since $dS_{21} \rightarrow 0$. Assuming that the dominant fluctuations are due to hot electron gas in the bridge, the NEP can be estimated taking into account only the thermal noise of the electron subsystem:

$$NEP = \sqrt{4k_B T_e^2 G} \quad (6).$$

The thermal conductance, G , can be defined from Equation (5) for $T_{bath} = T_{ph} = const$ as the derivative

$$G = dP_b / dT_e = 6 \cdot \Sigma \cdot V \cdot T_e^5 \quad (7)$$

yielding $G \approx 1.92 \cdot 10^{-11} \text{ W/K}$ and the intrinsic $NEP \approx 1 \cdot 10^{-17} \text{ W}/\sqrt{\text{Hz}}$ at electron temperature $T_e = 300 \text{ mK}$. This is good, but not a record figure, since the estimate is made for a relatively large bridge fabricated using convenient optical lithography. It is important to stress here that the above formulas (6) and (7) for the intrinsic NEP are characteristics of the absorber only while an ideal thermometer is assumed. To estimate the effect on NEP from the buffering low-noise amplifier (NEP_{LNA}), the conversion efficiency has to be used. That is why the impedance variation, which plays the role of internal thermometer, is of great importance. The formula for NEP_{LNA} from [8] can be evaluated in the following way:

$$NEP_{LNA} = \sqrt{\frac{k_B T_{LNA}}{2P_{bias}}} \times \frac{1}{S_{1/w}} = \sqrt{\frac{k_B T_{LNA} P_{bias}}{2}} \times \frac{1}{Gain} \quad (8).$$

Suggesting much smaller bridge, which can be fabricated using electron-beam lithography, for example, sized $0.25 \mu\text{m}$ by $0.25 \mu\text{m}$ by 25 nm ($V = 1.56 \cdot 10^{-21} \text{ m}^3$) and $T_{LNA} \approx 1 \text{ K}$ at 1.5 GHz , one may expect effective NEP essentially below $1 \text{ aW}/\sqrt{\text{Hz}}$ as presented in Figure 5.

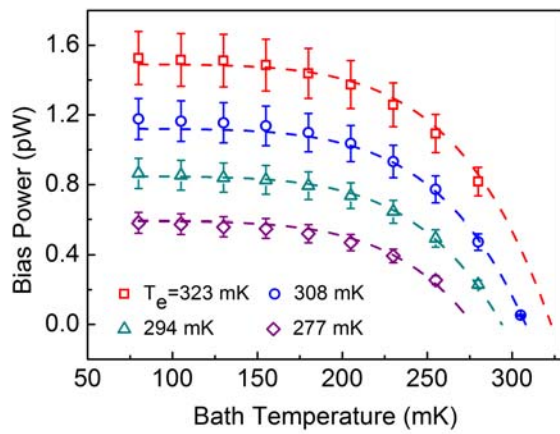


Figure 4. Fit of the electron-phonon model $P_B \sim T_e^6 - T_{ph}^6$ to experimental data at different T_e using method of steady Q -factor [17], $Q = Q(T_e) = const$ for each dashed curve. The absorbed bias power represents the absolute limit for the input signal power (saturation level).

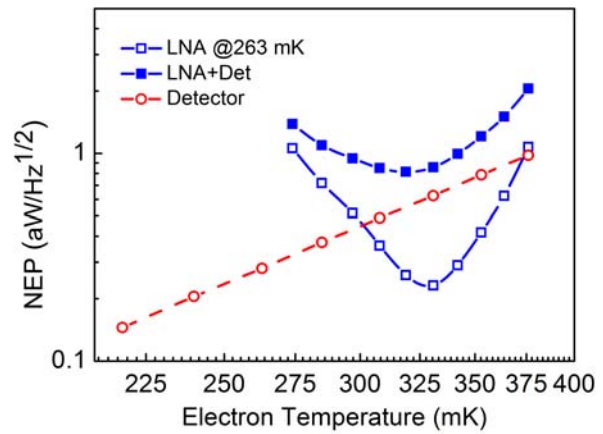


Figure 5. Estimated noise equivalent power for a small bridge fabricated using electron beam lithography: circles are by eq. (6) and (7). Effect of adding LNA: dark boxes. The open boxes corresponds to a low-noise amplifier ($T_{LNA} \approx 1$ K) using experimental specific thermal conductance eq. (7) and gain from eq. (4) for eq. (8).

3. Conclusions

The proof of the highly non-linear and microwave-readable impedance of RFTES device is an important step in the development of the FDM-operating bolometer array. It is demonstrated that the invasive effect of electron gas heating by microwaves opens possibility for setting an optimum electron temperature/response for each pixel independently. The efficient absorption of photons at 1.5 GHz suggests a useful range of the signal frequency from few GHz to, probably, tens THz. The predicted gain is beneficial for using the off-shelf semiconductor amplifiers. The present analysis, which is based on combination of the directly measured experimental data and acknowledged scaling techniques, allows to aim NEP down to and below $\approx 10^{-18}$ W/ $\sqrt{\text{Hz}}$ at relatively easy temperatures about 300 mK.

Acknowledgments

This work was supported, in the part of experimental study, by grant 17-19-01786 from Russian Science Foundation, and, in the part of numerical simulations, by Increase Competitiveness Program of NUST «MISiS» (№ K2-2014-025) from the Ministry of Education and Science of the Russian Federation.

References

- [1] Wellstood F C, Urbina C and Clarke J 1994 *Phys. Rev. B* **49** 5942-55
- [2] Karasik B S, McGrath W R, LeDuc H G and Gershenson M E 1999 *Supercond. Sci. Technol.* **12** 745-7
- [3] Gershenson M E, Gong D and Sato T 2001 *Appl. Phys. Lett.* **79** 2049
- [4] Karasik B S, Olaya D, Wei J et al. 2007 *IEEE Trans. Appl. Supercond.* **17** 293-7
- [5] Karasik B S and Cantor R 2011 *Appl. Phys. Lett.* **98** 193503
- [6] Lantinga T M, Cho H, Clarke J, Dobbs M, Lee A T, Lueker M, Richards P L, Smith A D and Spieler H G 2003 *Millimeter Submillimeter Detectors Astronomy* **4855** 172-81
- [7] Day D K, LeDuc H G, Mazin B A, Vayonakis A and Zmuidzinas J 2003 *Nature* **425** 817-21

- [8] Gao J 2008 *PhD thesis* California Institute of Technology
- [9] Zmuidzinis J 2012 *Annu. Rev. Condens. Matter Phys.* **3** 169
- [10] Lee S F, Gildemeister J M, Holmes W, Lee A T and Richards P L 1998 *Appl. Opt.* **37** 3391-97
- [11] Irwin K D and Hilton G C 2005 *Topics Appl. Phys.* **99** 63–149
- [12] Holland W 2006 *Proc. SPIE* **6275** 62751 E
- [13] Kuzmin A A, Shitov S V, Scheuring A, Meckbach J M, Il'in K S, Wuensch S H, Ustinov A V and Siegel M 2013 *IEEE Trans. THz Sci. Technol.* **3** 25-31
- [14] Kuzmin A A, A D Semenov, Shitov S V, Merker M, Wuensch S H, Ustinov A V and Siegel M 2017 *App. Phys. Lett.* **111** 042601
- [15] Shitov S V, Kuzmin A A, Merker M, Chichkov V I, Merenkov A V, Ermakov A B, Ustinov A V and Siegel M 2017 *IEEE Trans. Appl. Supercond.* **27** 4 2100805
- [16] Shitov S V, Abramov N N, Kuzmin A A, Merker M, Arndt M, Wuensch S H, Ilin K S, Erhan E V, Ustinov A V and Siegel M 2015 *IEEE Trans. Appl. Supercond.* **25** 3 2101704
- [17] Merenkov A V, Chichkov V I, Ermakov A B, Ustinov A V and Shitov S V 2018 *IEEE Trans. Appl. Supercond.* **28** 7
- [18] <https://nanoscienceoxinstcom/products/cryofree-dilution-refrigerators/triton>
- [19] <http://wwwawrcorpcom/products/ni-awr-design-environment/microwave-office>